Journal of Thermal Analysis and Calorimetry, Vol. 56 (1999) 603-610

A DILATOMETRIC INVESTIGATION OF THE THERMAL COMPACTION OF FERRITE POWDERS PREPARED BY COPRECIPITATION

V. Musat[1], *L. Rabardel*[2] *and E. Segal*[3]

[1]Department of Metallurgy and Materials Science, 'Dunarea de Jos' University
47 Domneasca, 6200 Galati, Romania
[2]I.C.M.C. Bordeaux, Château Brivazac-Av. Dr. A. Schweitzer, 33600 Pessac, France
[3]Department of Physical Chemistry, University of Bucharest, 13 Republicii, 70346 Bucharest
Romania

Abstract

The authors report on a non-isothermal kinetic investigation (at constant heating rate) of the sintering of manganese and nickel-zinc ferrite powders prepared by coprecipitation. The kinetic results point to the thermal compaction of the powders, which occurs mainly in the intermediate stage of sintering. A comparative study was performed in order to determine the influence of the sample characteristics (such as chemical nature, density and shape) and the heating rate on the kinetics and mechanism of the compaction.

Keywords: coprecipitation, ferrite, kinetics, sintering

Introduction

In a previous paper [1] we reported the results of an isothermal investigation of the sintering of a coprecipitated manganese ferrite powder [2], and subsequently performed a constant heating rate non-isothermal kinetic study [3, 4] on the sintering of coprecipitated (Ni,Zn)Fe_2O_4 and $MnFe_2O_4$ powders. The kinetic results obtained from the dilatometric data pointed to the thermal compaction of the powders, which occurs mainly in the intermediate stage of sintering [5]. The present paper relates to the influence of the sample characteristics (such as chemical nature, density and shape) and the heating rate on the kinetics and mechanism of the thermal compaction.

Experimental

Powders of $MnFe_2O_4$ prepared from MnO_2 and $FeSO_4{\cdot}7H_2O$ [2] and of (Ni,Zn)Fe_2O_4 obtained from an acid solution of $NiSO_4{\cdot}7H_2O$, $ZnSO_4{\cdot}6H_2O$ and $FeSO_4{\cdot}7H_2O$ through coprecipitation with 15% NaOH solution were used; the B.E.T. specific areas were 63 and 56 $m^2\ g^{-1}$, respectively.

The dilatometric measurements were carried out in air on cylindrical samples (9×5 mm) with Netzsch 402 ED differential dilatometer, and on toroidal samples (9×6×5 mm) with Harrop TDA equipment (Table 1). The heating rate are shown in Table 1. The linear contraction was measured in the generatrix direction.

1418–2874/99/ $ 5.00

Akadémiai Kiadó, Budapest
Kluwer Academic Publishers, Dordrecht

Table 1 Sample characteristics and experimental conditions

Sample symbol	Ferrite type	Geometrical shape of sample	Compaction pressure/ 10^8 Pa	Pressed sample density/ kg m^{-3}	Heating rate/ K min^{-1}
M1	$MnFe_2O_4$	cylindrical	1.1	2000±50	2
M2	$MnFe_2O_4$	cylindrical	3.5	2200±50	2
M3	$MnFe_2O_4$	toroidal	1.1	2000±50	5
M4	$MnFe_2O_4$	toroidal	3.5	2200±50	5
M5	$MnFe_2O_4$	cylindrical	3.5	2200±50	5
M6	$MnFe_2O_4$	cylindrical	3.5	2200±50	8
M7	$MnFe_2O_4$	cylindrical	3.5	2200±50	25
N1	$(Ni,Zn)Fe_2O_4$	cylindrical	3.5	2500±50	2
N2	$(Ni,Zn)Fe_2O_4$	cylindrical	3.5	2500±50	5
N3	$(Ni,Zn)Fe_2O_4$	cylindrical	3.5	2500±50	10
N4	$(Ni,Zn)Fe_2O_4$	toroidal	1.1	2150±50	3.5
N5	$(Ni,Zn)Fe_2O_4$	toroidal	1.1	2150±50	7

For a non-isothermal kinetic analysis of the compaction steps, the dilatometric curves were processed by means of the Young-Cutler [3] equation:

$$\left(\frac{\Delta L}{L_0}\right)^{n+1} = \frac{(n+1)ART^2 e^{-E/RT}}{aE} \qquad (1)$$

where $\Delta L/L_0$ is the relative change in sample length, n is the quasi-reaction order for compaction, A is the pre-exponential factor, E is the activation energy and a is the heating rate.

Results and discussion

Compaction of manganese ferrite powder

Analysis of the dilatometric data concerning the compressed powders of $MnFe_2O_4$ prepared by the wet method (samples M1–M7 in Table 1) led to the following findings:

The slope of the dilatometric curve is influenced considerably by the heating rate (Fig. 1), by the shape of the sample and, to a lesser extent, by the initial density (Figs 2 and 3).

The temperature ranges 200–350, 580–1000, 1000–1100 and 1100–1200°C relate to the first step, the intermediate steps and the final step of sintering, respectively.

The intermediate sintering (580–1000°C) exhibits a complex character, the change in the slope of the dilatometric curve being associated with a change in the

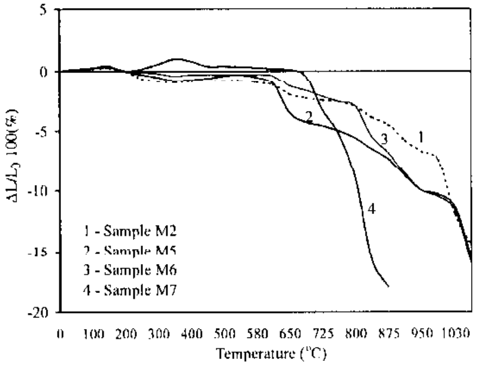

Fig. 1 Non-isothermal dilatometric curves of cylindrical $MnFe_2O_4$ samples for various heating rate

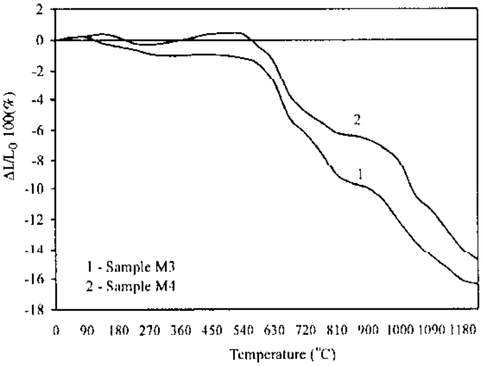

Fig. 2 Non-isothermal dilatometric curves of toroidal $MnFe_2O_4$ samples compressed at different pressures

compaction mechanism. This change is influenced by the heating rate, and by the form and initial density of the sample.

Increase of the heating rate shifts the compaction in the intermediate sintering towards lower temperatures in an unusual way. This is due to the structural changes which occur in the system Mn–Fe–O in the temperature range 450–1000°C, determined by the change in the oxidation state of the manganese ions; the decomposition of the spinel $MnFe_2O_4$ (a=8.405 Å) to α-Fe_2O_3 (a=3.17 Å) and Mn_2O_3 (a=3.70 Å), accompanied by a decrease in the lattice constant, acts in the same sense as the capillary forces towards contraction on a macroscopic scale. In the temperature range 900–1000°C, the increase in the lattice constant due to the crystallization of Mn_3O_4 and Fe_3O_4 spinels (which are actually ferrite precursors) acts against the sintering forces, braking the contraction. As the solid-state reactions are favoured by a low heating rate, their effect on compaction on a macroscopic scale is the more noticeable, the lower the heating rate is.

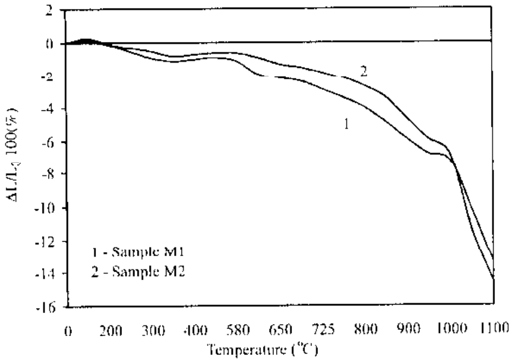

Fig. 3 Non-isothermal dilatometric curves of cylindrical $MnFe_2O_4$ samples compressed at different pressures

For the toroidal samples (Fig. 2), a more pronounced decrease of the contraction is observed until it vanishes in the temperature range 850–950°C. The phenomenon may be explained through the superposition of a braking effect in the direction of the generatrix (the direction in which the dilatometric measurements were made) and of the braking effect due to the spinel recrystallization. The braking of the contraction in the generatrix direction is due to a diffusion flux mainly in the radial direction from the outer convex surface to the inner concave surface of the tore [5, 6]. This effect is made clear if we compare the values of the relative linear contractions of the inner and outer diameters with the corresponding values of the contraction in the height of the tore.

Table 2 Values of the kinetic parameters for compaction of the cylindrical $MnFe_2O_4$ samples

Sample	Heating rate/ K min^{-1}	Parameter	Temperature range/°C			
			230–330	580–680	800–900	1030–1090
M2	2	n	0.68	1.4	3.8	5.2
		E/kJ mol^{-1}	44.8	134	298	368
		r*	0.9923	0.9947	0.9902	0.9928
M5	5	E/kJ mol^{-1}	47.3	73.5	273	372
		r*	0.9916	0.9922	0.9989	0.9968
M6	8	E/kJ mol^{-1}	82.5	125	218	362
		r*	0.9893	0.9932	0.9952	0.9978

r* – correlation coefficient of linear regression

An increase of the heating rate results in an increase in the compaction degree (Fig. 1). Through the decrease in the time for which the samples are at lower temperature (500–600°C), the contribution of the surface diffusion decreases too. This mass transport without compaction, specific to the initial step of sintering, causes a decrease in the specific area of the porous sample, and hence to a decrease in the moving force in the intermediate sintering [5]. This effect is more important for the powders obtained by a wet method (with high values of specific area) as the surface properties have a determinant role in compaction.

With regard to the dilatometric analysis data for the cylindrical samples M2, M5 and M6 (Table 1), a non-isothermal kinetic study was carried out. Via Eq. (1), from the slopes of the straight lines $\ln(\Delta L/L_0)$ *vs.* $\ln a$ for $T=ct$, the values of the kinetic parameter n corresponding to various compaction steps were estimated (Table 2). The different values of the parameter n reveal the change in the compaction mechanism on heating. The changes in the value and in the sign of the slopes of the straight lines $\ln(\Delta L/L_0)$ *vs.* $\ln a$ for $T=ct$ in the temperature range 680–800°C point to the competition between the two phenomena which control the compaction of the $MnFe_2O_4$ powder, namely the solid-state reaction and the decrease in the solid–gas interface. With these values of n, from the slope of the straight line $\ln(\Delta L/L_0)$ *vs.* $1/T$ at $a=ct$, the values of the activation energy according to Eq. (1) were calculated (Table 2).

As concerns the values of the activation energy, the following observations may be made:

The values corresponding to the thermal compaction in the temperature range 580–680°C decrease with heating rate increase, thereby confirming surface diffusion as the main mechanism in the initial compaction period.

We consider that the size of the crucibles (9×6×5 mm for the toroidal samples and 9×5 mm for the cylindrical samples) are small enough for significant alterations not to be introduced into the kinetic parameter values.

The compaction of the ferrite powders in the temperature range 200–350°C was made the subject of a kinetic investigation in which three methods used in non-isothermal kinetics [7] were applied. The experimental data were processed by means of the program VERSATILE [8]. The obtained values of the non-isothermal kinetic parameters are listed in Table 3.

The values of the reaction order between 0.7 and 0.8 indicate a contracting sphere mechanism for the compaction in the temperature range 200–350°C (accompanied by the removal of water). This mechanism was also indicated for the loss of water from these ferrite powders prepared by a wet method (the subject of a further paper). Obviously, taking into account a relative error of 10%, which affects the activation energy, the values of this parameter given in lines 1 and 2 of Table 3 do not differ significantly.

For the sintering of $MnFe_2O_4$ samples in the temperature range 600–1000°C, the shapes of the dilatometric curves are strongly influenced by the heating rate, showing that compaction and grain growth occur via different mechanisms. In this case, the compaction takes place in a multicomponent homogeneous system with the superposition of a solid-state reaction with single-step nucleation and diffusion-limited growth (600–680°C) or surface nucleation (750–800°C). In the temperature range 800–1000°C, the compaction of the samples is controlled by the volume diffusion.

In the temperature range 1000–1100°C, the compaction of the samples and the grain growth proceed through the same mechanism, namely grain boundary diffusion.

Table 3 Values of the non-isothermal kinetic parameters for compaction of the compressed $MnFe_2O_4$ samples in the temperature range 200–350°C

Sample	Coats-Redfern method				Flynn-Wall method				Modified Coats-Redfern method			
	E/ kJ mol^{-1}	A/ s^{-1}	n	r*	E/ kJ mol^{-1}	A/ s^{-1}	n	r*	E/ kJ mol^{-1}	A/ s^{-1}	n	r*
M2	45.9	25	0.75	0.9932	49.3	37	0.80	0.9928	48.1	37	0.75	0.9907
M5	46.4	41	0.70	0.9910	50.1	49	0.85	0.9943	48	36	0.80	0.9925
M6	98.6	$1.4\cdot10^5$	0.80	0.9889	102	$3.8\cdot10^5$	0.85	0.9891	100	2.9·104	0.85	0.9874

r* – correlation coefficient of linear regression

Table 4 Values of the kinetic parameters for compaction of the cylindrical $(Ni,Zn)Fe_2O_4$ samples

Sample	Heating rate/ K min^{-1}	Parameters	Temperature range/°C					
			600–680	700–780	800–900	900–1000	1030–1090	1095–1165
		n	1.8	2.1	3.0	3.3	5.0	5.3
N1	2	E/kJ mol^{-1}	154	250	223	210	381	159
		r*	0.9940	0.9948	0.9913	0.9950	0.9918	0.9893
N2	5	E/kJ mol^{-1}	115	252	237	198	385	160
		r*	0.9919	0.9997	0.9994	0.9899	0.9989	0.9901
N3	10	E/kJ mol^{-1}	64.3	236	235	189	368	148
		r*	0.9930	0.9909	0.9949	0.9966	0.9972	0.9921

r* – correlation coefficient of linear regression

Compaction of the nickel-zinc ferrite powder

Non-isothermal dilatometric curves corresponding to the compaction of the (Ni,Zn)Fe_2O_4 samples (N2–N5 in Table 1) are presented in Figs 4 and 5. Their analysis permits the following findings: The heating rate does not influence the form of the dilatometric curves (Fig. 4), indicating an identical mechanism of compaction and grain growth.

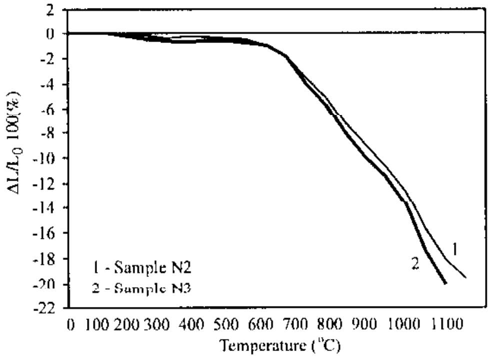

Fig. 4 Non-isothermal dilatometric curves of cylindrical (Ni,Zn)Fe_2O_4 samples

The linear contraction increases with increase of the heating rate (Figs 4 and 5). As the heating of (Ni,Zn)Fe_2O_4 occurs without a solid-state reaction, the increase in contraction with increase of the heating rate clearly shows that the surface diffusion acts in the first step of sintering of these powders.

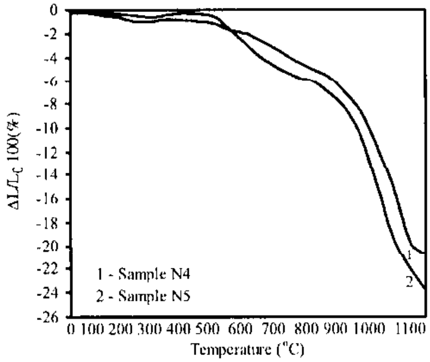

Fig. 5 Non-isothermal dilatometric curves of toroidal (Ni,Zn)Fe_2O_4 samples

For the toroidal samples, the dilatometric curves (Fig. 5) demonstrate a braking of the compaction in approximately the same temperature range as in the case of $MnFe_2O_4$ (850–950°C).

The values of the kinetic parameters n and E in the temperature range 600–1165°C, determined from the slope of the straight line $\ln(\Delta L/L_0)$ *vs.* $\ln a$, for $T=ct$, and the slope of the straight line $\ln(\Delta L/L_0$ *vs.* $1/T$ at $a=ct$, are given in Table 4.

The data in Table 4 show that:

– the activation energy of compaction in the temperature range 600–680°C decreases with increase of the heating rate, as a result of the decrease in surface diffusion at high heating rates;

– the value of parameter n changes continuously, indicating the continuous change in the mechanism which controls compaction and grain growth;

– the activation energies of compaction in the temperature range 1030–1090°C are approximately equal at all heating rates and close to that corresponding to the compaction of $MnFe_2O_4$.

Conclusions

The kinetic parameters and the mechanism of thermal compaction of $MnFe_2O_4$ and $(Ni,Zn).Fe_2O_4$ powders prepared by wet methods were followed in the temperature ranges 200–350, 600–1000 and 1030–1090°C.

References

1 E. Segal, M. Brezeanu and V. Bujoreanu Musat, Thermochim. Acta, 221 (1993) 85.
2 V. Musat, E. Segal, M. Brezeanu, R. Salmon and J. J. Videau, Thermochim. Acta, 288 (1996) 221.
3 W. S. Young and I. B. Cutler, J. Amer. Ceram. Soc., 53 (1970) 659.
4 J. L. Woolfrey and M. J. Bannister, J. Amer. Ceram. Soc., 55 (1972) 390.
5 L. M. Letjuk and G. I. Zuravlev, Khimiya i Tekhnologiya Ferritov, Khimiya, Leningrad 1983.
6 F. F. Lange, J. Amer. Ceram. Soc., 67 (1984) 83.
7 E. Segal and D. Fatu, Introduction to Non-isothermal Kinetics, Publishing House of Romanian Academy, Bucharest 1984.
8 E. Segal and E. Coseac, Rev. Romaine Chem., 34 (1989) 287.